Solid State Phenomena
ISSN: 1662-9779, Vol. 297, pp 31-50

Submitted: 2019-01-22
Revised: 2019-03-11
Accepted: 2019-03-30
Online: 2019-09-17

Constitutive Modelling of an Industrial Rolled Sheet for a DIN 1623 St14 (DC04) Steel

B. Regaiguia[1,2,a], O. Chahaoui[1,b*], S. Boulahrouz[1,c], N. Brinis[1,d], M. L Fares[2,e]

[1]Engineering Sciences and Advanced Materials Laboratory (ISMA), Laghrour-Abbes University of Khenchela, P.O. Box 1252, 40004, Algeria

[2]Metallurgy and Engineering Materials, Badji-Mokhtar University of Annaba, P.O. Box 12, 23000, Algeria.

[a]bregaiguia@yahoo.fr, [*b]oualid.chahaoui@yahoo.fr, [c]boulahrouz_salim@yahoo.fr, [d]naoel.brinis@gmail.com, [e]fareslamine@yahoo.fr

Keywords: Constitutive model, DIN 1623 St14 steel, sheet metal forming, plastic anisotropy, orthotropic yield criterion, isotropic hardening function.

Abstract The comprehension of the anisotropy impacts on mechanical properties of the rolled steel sheets was investigated using a non-quadratic anisotropic yield function. In this study, experimental and modelling determination of behavior of an industrial rolled sheets for a DIN 1623 St14 steel were carried out. The yield stresses and Lankford *r*-values in uniaxial were experimentally determined but the balanced biaxial tension stress states and *rb* were assumed. The parameters of the associated yield equation, derived from the three orthotropic yield functions proposed by Hill48 and Yld2000-2d, were determined. Predictions and the evolution of normalized yield stress and normalized Lankford parameters (plastic strain ratio) obtained by the presented investigative are considered. In order to describe the path of equivalent plastic behavior, the isotropic hardening function is described using the following various empirical standard formulae based on: Hollomon, Ludwick, Swift and Voce model.

Introduction

Forming is the most widely used sheet metal operation used for manufacturing various sheet metal components across the actual industry. It is a well-known fact that the drawability properties of forming sheet (e.g. occurrence Earing in Deep Drawing under Various Conditions, or roping) largely depend on anisotropy induced by rolling process. More often than not the manufacturing process of the metal alloy induces certain preferred crystallographic orientations and therefore, most metals exhibit a crystallographic texture [1], for two reasons: (i) continuous recrystallization occurs during hot working, which precludes randomization of grain orientations, and (ii) no phase transformation occurs upon cooling. Furthermore, such textures cannot be entirely eliminated or even modified by subsequent cold rolling and/or heat treatments [2].

The rolling sheets are characterized by the presence of three mutually orthogonal planes of orthotropic symmetry. It is notable that the rolling process promotes the existence of induced anisotropy, which greatly influences the drawability properties and formability of sheet metals to the desired dimensions and shape. This is especially true for aluminium alloys and ferritic steels, which exhibit strong crystallographic textures after hot rolling [3, 4]. For this purpose and in aim to describe the anisotropic behavior of materials, several such functions (quadratic and non-quadratic) have been proposed. Initially, Hill [5], which is a simple modification of the standard von Mises plasticity to give a quadratic yield function mainly based on the assumption of an associated flow rule. Another isotropic approach of yield functions introduced by Hosford [6] and was extended to a planar anisotropic model by Barlat et al. [7- 12]. As for the constitutive law, a more flexible and adaptable model is the non-quadratic anisotropic yield function, Yld2000-2d, was used to describe the initial anisotropic yield surface along with the isotropic hardening law for the yield surface evolution. This is having 8 material parameters which can be identified by the yield stresses and strain ratios in three

uniaxial cases, RD (0°), DD (45°) and TD (90°) and one equibiaxial tension case with a varying cross-section [11]. Yield functions can involve a several anisotropy coefficients for a material. The identification of these parameters requires usually high number mechanical tests in different directions following loading paths. To ensure a certain precision of parameters, the number of experimental data should not be lower than the number of material parameters considered in the identification operation [13].

St14 steel (DIN 1623) is commonly applied in the sheet metal forming industries such as automobile manufacturing, rolling stock, aerospace for of its remarkable formability and also its low price [14]. In this paper, phenomenological material model of DIN 1623 St14 steel was investigated by using Yld2000-2d model with variation of stress ratio and the data obtained from the experiment.

The remainder of this investigative work is structured as follows. Section 1, a basic mathematical description of the anisotropic behavior of a homogeneous rolled sheet, expressed in accordance with the Hill's formalism and improving Barlat's Yld2000-2d yield function of generalized materials, is presented. In Section 2 describes experiments that were carried out to determine the mechanical characteristics of the material according to the needs of the analysis, since mechanical experiments are used to provide comparison with theoretical results. Then, in Section 3, describes the isotropic hardening for a metal sheet with four classical laws using curve fitting for Stress-Strain experimental data. Finally, for a better prediction, the experimental plastic work contours are obtained according to the plastic work equivalent theorem, von Mises, Hill48 and Yld2000-2d yield functions are compared with the experimental contours is employed in Section 4.

Notation

RD, TD, DD,ND	Rolling, transverse, diagonal and normal directions of the sheet
F, G, H, L, M, N	Anisotropy parameters of the Hill orthotropic yield function
k	Material constant (k=8 for FCC materials and k=6 for BCC materials)
S'_1, S'_2	First linear transformations on the stress deviator
S''_1, S''_2	Second linear transformations on the stress deviator
S_1, S_2	Principal stress deviators
α_1-α_8	Anisotropy parameters in YLD2000-2d
$r(\theta)$	Strain rate ratio at an angle θ in the sheet plane (Lankford value)
θ	Angle between a direction in the sheet plane and the rolling direction RD
σ_{ij}	Stress tensor components
σ_0	Equivalent flow stress
$\sigma_{ref}=\sigma_0$	The reference yield stress: Uniaxial tensile stress in rolling direction
$\sigma(\theta)$	Yield stress of the tensile test specimen under uniaxial load
σ_b	Equibiaxial stress
r_b	Equibiaxial *r*-value
$\dot{\varepsilon}_{ij}$	Strain rate tensor components
σ_t, ε_t	True Stress and true strain rate
K_h, K_l, K_s, σ_{sat} ,	Parameters of Hollomon, Ludwick, Swift and Voce isotropic hardening law
nh, nl, ns, nv	Hardening components
ε_0	Strain shift parameter of Swift
$\dot{w}^p$	The plastic stress-work density
E	Young's modulus

2. Phenomenological Models

In this section, two yield criteria, which were used to predict the anisotropic plastic behaviour of the **DIN 1623 St14 steel** sheet.

2.1 Hill's 48 yield criteria

The first stress yield function describing the anisotropic behavior of rolled sheets, was the homogeneous quadratic criterion proposed by Hill [5, 15], insensitive to Bauschinger effect and to hydrostatic pressure involving six independent parameters. Considering (RD: the rolling direction, TD: the transverse direction and ND: the normal direction) the three orthotropic directions, it can be written in the form

$$f(\sigma_{ij}) = F(\sigma_{22}-\sigma_{33})^2 + G(\sigma_{33}-\sigma_{11})^2 + H(\sigma_{11}-\sigma_{22})^2 + 2L\sigma_{23}^2 + 2M\sigma_{13}^2 + 2N_{12}^2 = \sigma_0^2 \tag{1}$$

The anisotropic coefficients *F*, *G*, *H*, *L*, *M* and *N* can be derived from texture components (see also [2]) or usually determined from mechanical tests (i.e.; uniaxial tensile as well as simple shearing). Whenever, in plane stress state (i.e.; $\sigma_{33}=\sigma_{13}=\sigma_{23}=0$, and $\sigma_{11},\sigma_{22},\sigma_{12}\neq 0$) , equation 1 can be reduced to

$$F\sigma_{22}^2 + G\sigma_{11}^2 + H(\sigma_{11}-\sigma_{22})^2 + 2N\sigma_{12} = \sigma_0^2 \tag{2}$$

If σ_0^1, σ_0^2 and σ_0^3 are the yield stresses in uniaxial tension along the axes RD, TD, and ND, respectively:

$$G+H = 2\left(\sigma_0/\sigma_0^1\right)^2 \qquad F+H = 2\left(\sigma_0/\sigma_0^2\right)^2 \qquad F+G = 2\left(\sigma_0/\sigma^3\right)^2 \tag{3}$$

If σ_0^{23}, σ_0^{13} and σ_0^{12} are the simple shear stresses along the anisotropy axes:

$$L = \left(\sigma_0/\sigma_0^{23}\right)^2 \qquad M = \left(\sigma_0/\sigma_0^{13}\right)^2 \qquad N = \left(\sigma_0/\sigma_0^{12}\right)^2$$

F, G, H and *N* can be related to experimental r-values and/or yield stresses. The following possibilities are considered:

i) Input data is $\sigma_0,\sigma_{45},\sigma_{90},\sigma_b$ [16].

$$F = \frac{1}{2}\left[\frac{\sigma_0^2}{\sigma_{90}^2}+\frac{\sigma_0^2}{\sigma_b^2}-1\right] \qquad G = \frac{1}{2}\left[1-\frac{\sigma_0^2}{\sigma_{90}^2}+\frac{\sigma_0^2}{\sigma_b^2}\right]$$
$$H = \frac{1}{2}\left[1+\frac{\sigma_0^2}{\sigma_{90}^2}-\frac{\sigma_0^2}{\sigma_b^2}\right] \qquad N = \frac{1}{2}\left[\frac{4\sigma_0^2}{\sigma_{45}^2}-\frac{\sigma_0^2}{\sigma_b^2}\right] \tag{4}$$

i) Input data is r_0, r_{45}, r_{90} [17].

$$F = \frac{r_0}{r_{90}(1+r_0)} \qquad G = \frac{1}{(1+r_0)}$$

$$H = \frac{r_0}{(1+r_0)} \qquad N = \frac{(1+2r_{45})(r_0+r_{90})}{2r_{90}(1+r_0)} \tag{5}$$

ii) Input data is $\sigma_0, \sigma_{45}, \sigma_{90}, r_{90}$ [18].

$$F = \frac{2\sigma_0^2}{\sigma_{90}^2(1+r_{90})} \qquad G = 2 - \frac{2\sigma_0^2 r_{90}}{\sigma_{90}^2(1+r_{90})}$$
$$H = \frac{2\sigma_0^2 r_{90}}{\sigma_{90}^2(1+r_{90})} \qquad N = \frac{4\sigma_0^2}{\sigma_{45}^2} - 1 + \frac{\sigma_0^2(r_{90}-1)}{\sigma_{90}^2(1+r_{90})} \tag{6}$$

Note that all these variants imply $\sigma_{ref} = \sigma_0$

Since formability of any sheet is characterized by $\sigma(\theta)$ mechanical parameter that is primarily related to the size and shape of grains, drawability is usually related to the *r-value*, which is defined as the ratio of the true strains in the width and in the thickness directions, respectively. Based on the Hill quadratic criterion as well as on the associated flow rule according to normality principle, relationships determining mechanical and anisotropic parameters are (See details in Appendix 1):

$$\sigma(\theta) = \frac{\sigma_0}{\left(F\sin^4\theta + G\cos^4\theta + H\cos^2 2\theta + 2N\sin^2\theta\cos^2\theta\right)^{1/2}} \tag{7a}$$

$$r(\theta) = \frac{H\cos^2 2\theta - (F+G-2N)\cos^2\theta\sin^2\theta}{F\sin^2\theta + G\cos^2\theta} \tag{7b}$$

2.2 Yld2000-2d yield criteria.

Barlat et al [11] proposed a non-quadratic anisotropic plastic potential model for metals, which is also very successful for steel. Equation 8 expresses the Yld2000-2d yield criteria in terms of the principal stress deviators tensor:

$$f(\sigma_{ij}) = \Phi = \left|S_1' - S_2'\right|^k + \left|2S_2'' + S_1''\right|^k + \left|2S_1'' + S_2''\right|^k = 2\sigma_0{}^k \tag{8}$$

For the anisotropic case, the linear transformations reduce to

$$\begin{bmatrix} S_{11}' \\ S_{22}' \\ S_{12}' \end{bmatrix} = \begin{bmatrix} C_{11}' & C_{12}' & 0 \\ C_{21}' & C_{22}' & 0 \\ 0 & 0 & C_{66}' \end{bmatrix} \begin{bmatrix} s_{11} \\ s_{22} \\ s_{12} \end{bmatrix}, \qquad \begin{bmatrix} S_{11}'' \\ S_{22}'' \\ S_{12}'' \end{bmatrix} = \begin{bmatrix} C_{11}'' & C_{12}'' & 0 \\ C_{21}'' & C_{22}'' & 0 \\ 0 & 0 & C_{66}'' \end{bmatrix} \begin{bmatrix} s_{11} \\ s_{22} \\ s_{12} \end{bmatrix} \tag{9}$$

Or, the transformation can also apply on the Cauchy stress tensor σ as

$$\begin{cases} S' = C'S = C'T\sigma = L'\sigma \\ S'' = C''S = C''T\sigma = L''\sigma \end{cases} \tag{10}$$

In this case the first and the second modified principal deviatoric stresses $S_{1,2}'$, $S_{1,2}''$ in plane sheet can be shown as:

$$S'_{1,2} = \frac{1}{2}(S'_{11} + S'_{22}) \pm \frac{1}{2}\sqrt{(S'_{11} - S'_{22})^2 + 4S'^2_{12}}$$
$$S''_{1,2} = \frac{1}{2}(S''_{11} + S''_{22}) \pm \frac{1}{2}\sqrt{(S''_{11} - S''_{22})^2 + 4S''^2_{12}} \quad (11)$$

In the previous equations, *C'* and *C''* are linear transformation matrices. Where the transformation matrix, *T*, is

$$T = \frac{1}{3}\begin{bmatrix} 2 & -1 & -1 & 0 & 0 & 0 \\ -1 & 2 & -1 & 0 & 0 & 0 \\ -1 & -1 & 2 & 0 & 0 & 0 \\ 0 & 0 & 0 & 3 & 0 & 0 \\ 0 & 0 & 0 & 0 & 3 & 0 \\ 0 & 0 & 0 & 0 & 0 & 3 \end{bmatrix} \overset{\text{Plane}}{=} \begin{bmatrix} 2/3 & -1/3 & 0 \\ -1/3 & 2/3 & 0 \\ 0 & 0 & 1 \end{bmatrix} \quad (12)$$

The tensors *L'* and *L''* representing linear transformations of the stress tensor are.

$$L_{ij} = \begin{bmatrix} L_{11} & L_{12} & L_{13} & 0 & 0 & 0 \\ L_{21} & L_{22} & L_{23} & 0 & 0 & 0 \\ L_{31} & L_{32} & L_{33} & 0 & 0 & 0 \\ 0 & 0 & 0 & L_{44} & 0 & 0 \\ 0 & 0 & 0 & 0 & L_{55} & 0 \\ 0 & 0 & 0 & 0 & 0 & L_{66} \end{bmatrix} \overset{\text{Plane}}{=} \begin{bmatrix} L_{11} & L_{12} & 0 \\ L_{21} & L_{22} & 0 \\ 0 & 0 & L_{66} \end{bmatrix} \quad (13)$$

Therefor $L_{1m} + L_{2m} + L_{3m} = 0$ for $m = 1, 2, 3$.

For convenience in the calculation of the anisotropy parameters, the coefficients of *L'* and *L''* can be expressed as follows:

$$L' = \begin{bmatrix} L'_{11} \\ L'_{12} \\ L'_{21} \\ L'_{22} \\ L'_{66} \end{bmatrix} = \begin{bmatrix} \frac{2}{3} & 0 & 0 \\ \frac{-1}{3} & 0 & 0 \\ 0 & \frac{-1}{3} & 0 \\ 0 & \frac{2}{3} & 0 \\ 0 & 0 & 1 \end{bmatrix} \begin{bmatrix} \alpha_1 \\ \alpha_2 \\ \alpha_7 \end{bmatrix}, \qquad L'' = \begin{bmatrix} L''_{11} \\ L''_{12} \\ L''_{21} \\ L''_{22} \\ L''_{66} \end{bmatrix} = \frac{1}{9}\begin{bmatrix} -2 & 2 & 8 & -2 & 0 \\ 1 & -4 & -4 & 4 & 0 \\ 4 & -4 & -4 & 1 & 0 \\ -2 & 8 & 2 & -2 & 0 \\ 0 & 0 & 0 & 0 & 9 \end{bmatrix} \begin{bmatrix} \alpha_3 \\ \alpha_4 \\ \alpha_5 \\ \alpha_6 \\ \alpha_8 \end{bmatrix} \quad (14)$$

The sheet rolled is strongly anisotropic, to describe this property, it is necessary to identify eight independent coefficients of anisotropy such as: $\alpha_1 \ldots\ldots \alpha_7$ and α_8 where they reduce to unite in the simple isotropic case. The eight unknown anisotropy coefficients of the Yld2000-2d yield function were obtained using the eight experimental material data (σ_0, σ_{45}, σ_{90}, σ_b, r_0, r_{45}, r_{90}, r_b) Where the yield stresses and *r*-values (width-to-thickness strain ratio of tension specimen) measured in three

different directions of the sheet from uniaxial tension tests. r_b is the equibiaxial Lankford and σ_b is equibiaxial flow stress.

A nonlinear system of seven equations of the seven unknowns is recommended to be solved using the Newton-Raphson method to determine the α_i parameters (see appendix2) and obtaining the numerical solution are given in [19-21]. The reference yield stress is $\sigma_{ref} = \sigma_0$. The rotation rules of stress components from the specimen reference to the sheet axes in uniaxial test are given as

$$\begin{cases} \sigma_{11} = \sigma(\theta)\cos^2\theta \\ \sigma_{22} = \sigma(\theta)\cos^2\theta \\ \sigma_{12} = \sigma(\theta)\sin\theta\cos\theta \end{cases} \tag{15}$$

$\sigma(\theta)$: is the yield stress of specimen under uniaxial tensile test.

A directional *r*-value $r(\theta)$, associated with the orientation angle θ in plane sheet can be calculated from

$$r(\theta) = \frac{\dot{\varepsilon}_{yy}}{\dot{\varepsilon}_{zz}} = -\frac{(\frac{f(\sigma_{ij})}{\partial\sigma_{11}}).\sin^2\theta - (\frac{f(\sigma_{ij})}{\partial\sigma_{12}}).\sin 2\theta + (\frac{f(\sigma_{ij})}{\partial\sigma_{22}}).\cos^2\theta}{\frac{f(\sigma_{ij})}{\partial\sigma_{11}} + \frac{f(\sigma_{ij})}{\partial\sigma_{22}}} \tag{16}$$

Where : $$f(\sigma_{ij}) = \left(\frac{\Phi}{2}\right)^{1/K} = \left(\frac{\Phi' + \Phi''}{2}\right)^{1/K}$$

3. Experimental Work and Material Properties

The base material examined in the present investigation is a DIN 1623 St14 steel (ASTM A620; NE 10130-2006). It was supplied by Algerian Tractors Company (ATC) as 1.35 mm annealed rolled sheet with a chemical composition listed in table1.

Table 1. Chemical composition of examined DIN 1623 St14 steel (in wt. %).

C	Si	Mn	P	S	Mo	Al	Cu	Ti	W	N	Sb
0.06	0.03	0.19	0.012	0.011	0.01	0.039	0.051	0.004	0.06	0.002	0.003

All tests were performed using a Zwick/Roell 50 KN testing machine. Uniaxial tensile tests were carried out to determine quasi-static stress-strain curve and *r-values*. The tests were performed using standard specimens at a strain rate of 0.008m/s to obtain the quasi-static material response for tension. The dimensions and the sheet sample are shown in figure 1. Specimens prepared along the angle 0˚, 45˚ and 90˚ to the rolling direction (RD) were investigated and flow stresses for each loading direction were obtained. The experimental mechanical parameters of the material i.e., yield stress (σ_e), maximum tensile stress (σ_m), the Poisson's ratio (ν) and *r-values* at 0, 45 and 90° to the rolling direction (RD).

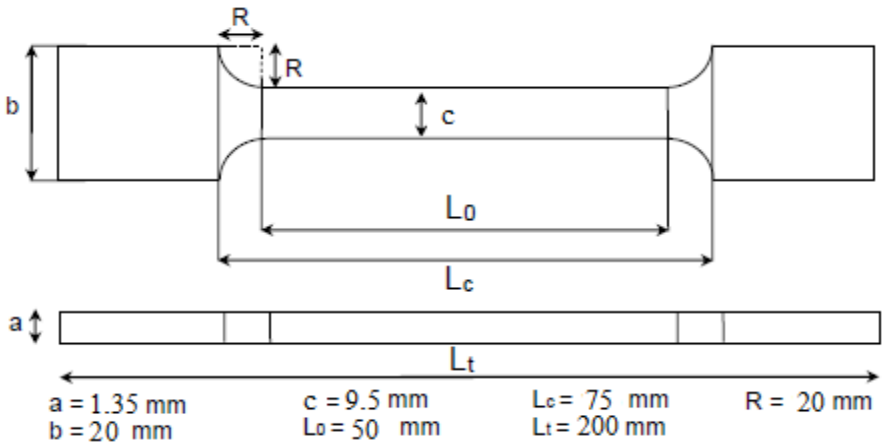

Fig.1. Dimensions of the specimen

For reproducibility, three plate tensile specimens were machined from the as-received sheet by fixing the angle θ between tensile and rolling directions ranging from 0° to 90 (0°=RD, 30°,45°=DD,60° and 90°=TD). The anisotropic coefficients of this rolled sheet were also calculated for the 18% pre-strain level and the results were tabulated in table 2.

Table 2. Mechanical Property for DIN 1623 St 14 steel in three directions

Direction	ν	σ_e *(0.2% offset) (MPa)*	σ_m *(MPa)*	r
0°		258	365	1.8
30°	0.3	254	380	
45°		263	380	1..5
60°		257	374	
90°		251	367	2.13

Figure 2 shows the uniaxial hardening curves for specimens extracted at three different orientations (RD, DD and TD). The yield curves in TD and RD are even crossing each other.

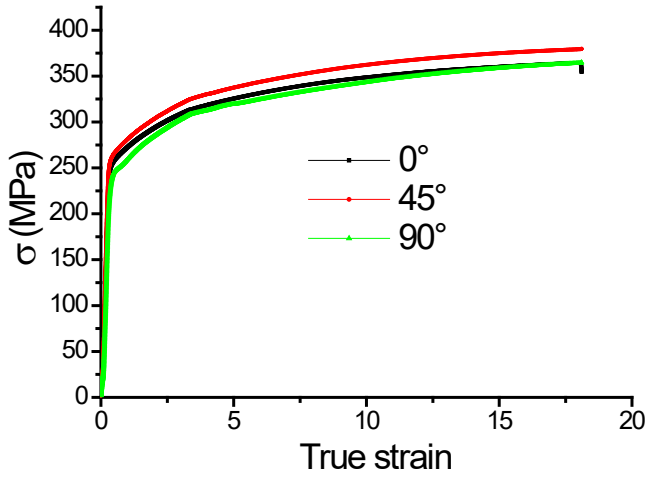

Fig. 2. Hardening curves for St 14 steel

The normalized flow stresses (yield stress) and *r*-value for different directions are presented in table 3. Yield stresses for each direction were then normalized by the uniaxial yield stress for the rolling direction.

Table 3. The normalized tensile yield stress by the rolling direction uniaxial yield stress

Yield stress	σ_0/σ_u	σ_{30}/σ_0	σ_{45}/σ_u	σ_{60}/σ_0	σ_{90}/σ_u	σ_b/σ_u
	1	0.984	1.019	0.996	0.97	0.985
r-value	r_0/r_0		r_{45}/r_0		r_{90}/r_0	r_b
	1		0.84		1.18	1

Note that the equibiaxial yield stress σ_b and the corresponding r_b-value were assumed in this work. Thus, $\sigma_b = (\sigma_0 + \sigma_{90})/2$ and $r_b = 1$.

The four anisotropic coefficients of Hill's 1948 (*F, G, H* and *N*) in plane sheet were calculated from equation 4 and all independent coefficients α_i were computed using the matlab code of Newton-Raphson iteration method. The Values of anisotropic parameters used in calculations for the DIN 1623 St14 steel are tabulated in table 4.

Table 4. Calculated anisotropy parameters for the DIN 1623 St14 steel to 3 digits for writing convenience

DIN 1623 St14 steel	Hill48	F		G		H		N	
		0.485		0.542		0.514		1.410	
	YLD2000-2d K=6	α_1	α_2	α_3	α_4	α_5	α_6	α_7	α_8
		0.968	1.173	1.141	0.970	0.978	1.049	1.020	0.848

Corresponding results are displayed in figure 3 for both normalized mechanical parameters $\sigma\ \theta$) and *r* (θ). Figure (3a-b) illustrates the influence of the experimental results of the normalized yield stress $\sigma\ \theta$) and the plastic strain ratio *r* (θ) in the sheet plane showing the angular dependence. During this investigation, it was found that the Yld2000-2d and Hill-48 criterions are significantly different where an important divergence is observed for the different directions in plane sheet for the normalized yield stress σ (θ) figure 3(a). Accordingly, it is possible to quantify the impact of orientation from 45° to 90° (in the first quadrant) on the departure from anisotropy between two functions for the global behavior *r (θ)-values* figure 3 (b). Additionally, the corresponding yield Loci of the materials that are obtained for the studied yield criteria were plotted in figure 3(c). The flow stresses $\sigma(\theta)$ and the Lankford *r-values* $r(\theta)$ deducted from Yld2000-2d also agree with experimental data very well. It should be noted that from the results figure 3(c), the Yld2000-2d yield function with an exponent of 6 is capable of reproducing the plastic deformation behavior.

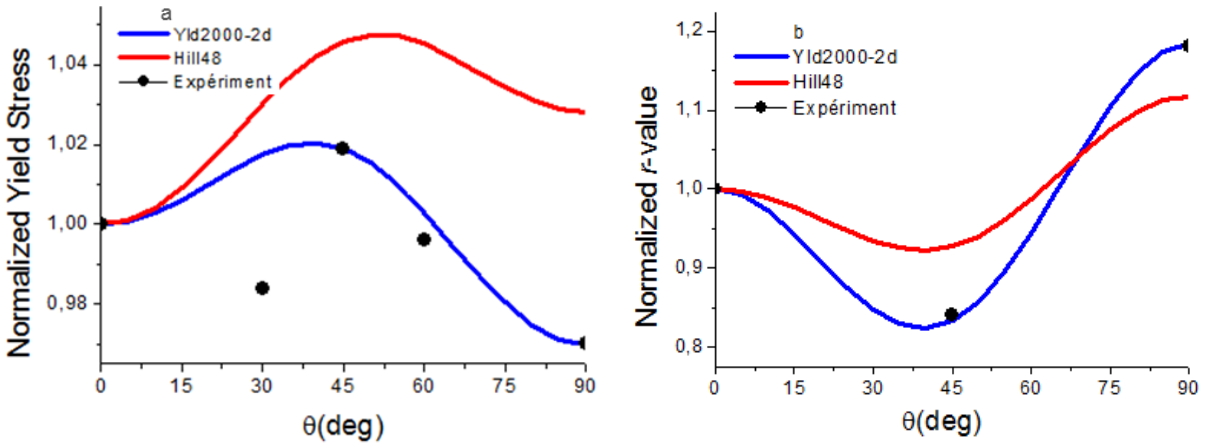

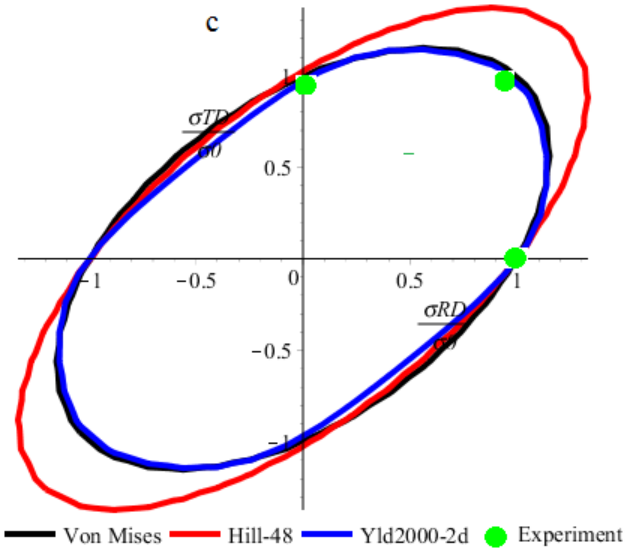

Fig.3. Distribution of the uniaxial mechanical parameters for DIN 1623 St14 steel (a) Normalized yield stress (b) Plastic strain ratio and in (c) Experimental data representing the initial yield surface and Predicted yield surface contours with Hill-48, YLD-2000-2d and isotropic behavior

3.1 Curve fitting for Stress-Strain experimental data with isotropic hardening model

The flow stress equation is related with stress and strain data in order to describe the path of strain behavior of DIN 1623 St14 steel. The isotropic hardening function is described using the following various empirical standard formulae based on: Hollomon, Ludwick, Swift and Voce model in the rolling direction.

- The Hollomon hardening law is: $\sigma_t = K_h\ \varepsilon_t^{nh}$
- The Ludwick hardening law is: $\sigma_t = \sigma_0 + K_l\ \varepsilon_t^{nl}$
- The Swift hardening law is: $\sigma_t = K_s\ (\varepsilon_0 + \varepsilon_t)^{ns}$ and $\varepsilon_0 = \sigma_0 / E$
- The Voce hardening law is: $\sigma_t = \sigma_{Sat} - (\sigma_{Sat} - \sigma_0)\exp(-nv\,\varepsilon_t)$

In order to quantitatively evaluate the theoretical yield stress-strain relations, using an error function for each stress-strain relation:

$$\delta = \sqrt{\frac{1}{n}\sum_{i=1}^{n}\left(\frac{\sigma^{i}{}_{Theoritical} - \sigma^{i}{}_{Experimental}}{\sigma^{i}{}_{Experimental}}\right)^{2}} \tag{17}$$

Where n is the number of the experimental points; $\sigma^{i}{}_{Theoritical}$ and $\sigma^{i}{}_{Experimental}$ are the experimental stress and the corresponding theoretical stress, respectively. K_h, K_l, K_s, σ_{sat}, n_h, n_l, n_s, and n_v were obtained by fitting data $(\sigma_t, \varepsilon_t)$ in the uniaxial tensile test along the rolling direction (0°) and the results are presented in table 5.

Table 5. Fitting data of the four hardening laws

Hollomon		Ludwick		Swift		Voce	
K_h [MPa]	*531.71*	*Kl* [MPa]	*567.48*	*Ks* [MPa]	*551.7*	σ_{sat} [MPa]	*444.71*
nh	*0.137*	*nl*	*0.644*	*ns*	*0.153*	*nv*	*12.77*

In figure 4, the experimentally measured stress-strain curve and the fit by the four laws, which were utilized for St14 steel. It is shown that a good fit is achieved firstly by the Ludwick, thereafter by Voce, Swift and Hollomon model respectively. Therefore, the Ludwick law is adopted in this work.

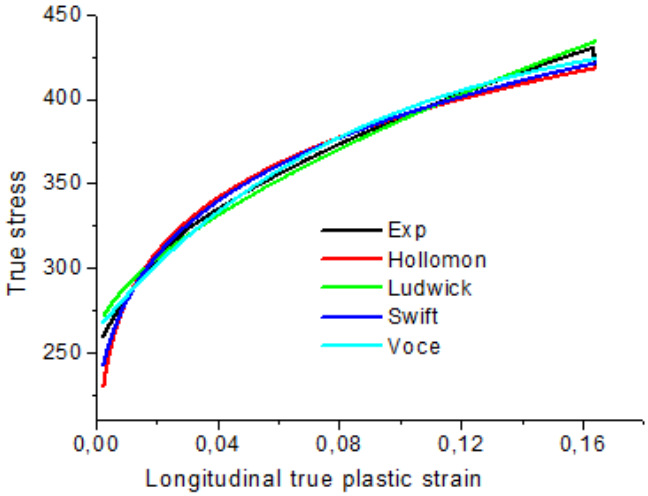

Fig. 4. Fitting of experimental hardening curve with different hardening models

3.2 The plastic work contours

The notion of the contour of plastic work dissipated and corresponding to the stress space was used to quantitatively evaluate the work hardening behavior of the test material under biaxial tension, more especially when the shape of successive yield loci varies. The evaluation of the plastic work contours was experimentally determined according to the plastic work equivalent theorem. Macroscopically, the stress-strain curves obtained from a uniaxial tensile test along $\theta = (0°, 45°, 90°)$ [22- 25]. The corresponding plastic work w^p is computed according to equation 18.

$$\begin{cases} w^p(\theta) = \sigma(\theta)\,\varepsilon_\theta^p \\ w^p(0°) = \int \sigma(0°)\, d\varepsilon_0{}^p \\ w^p(45°) = \int \sigma(45°)\, d\varepsilon_{45}{}^p \\ w^p(90°) = \int \sigma(90°)\, d\varepsilon_{90}{}^p \end{cases} \tag{18}$$

The longitudinal equivalent plastic strain-rate ε^p for three orientations (0°,45°,90° and equi-biaxial direction), is conjugate to each yield stress σ_0 with respect to the rate of plastic work per unit volume w^p. Ludwick's hardening equations were used for calculating the yield stress in terms of the equivalent plastic strain until 100%. The directional hardening curves in three direction (RD, DD, TD and equi-biaxial direction) are given by equation 19:

$$\begin{cases} \sigma_0(\varepsilon_0{}^p) = 259 + 567.18\,(\varepsilon_0{}^p)^{0.644} \\ \sigma_{45}(\varepsilon_{45}{}^p) = 263 + 590.23\,(\varepsilon_{45}{}^p)^{0.611} \\ \sigma_{90}(\varepsilon_{90}{}^p) = 251 + 644.30\,(\varepsilon_{90}{}^p)^{0.667} \\ \sigma_b(\varepsilon_i{}^p) = (\sigma_0(\varepsilon_i{}^p) + \sigma_{90}(\varepsilon_i{}^p))/2 \end{cases} \tag{19}$$

The plastic strain and plastic work density of DIN 1623 St14 steel sheet are plotted in figures 5 and 6, respectively.

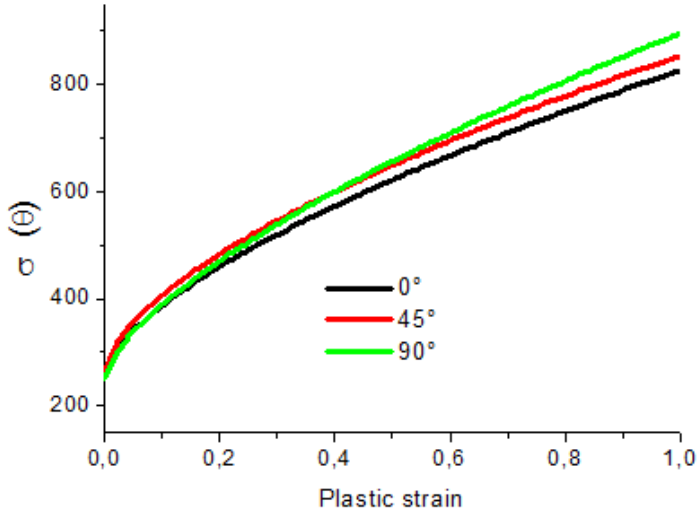

Fig.5. The hardening curves from different testing in terms of 100% of plastic strain

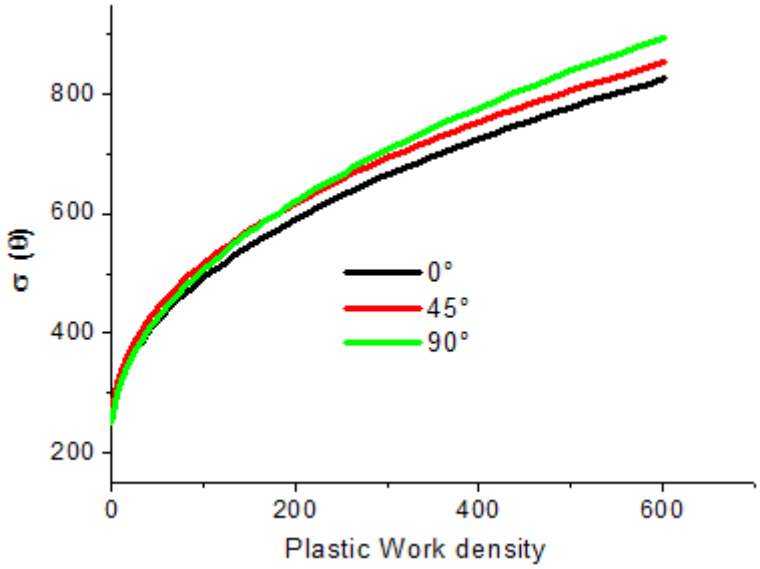

Fig. 6. The hardening curves from different testing.in terms of plastic work density

Directional uniaxial tensile test and the assuming of equibiaxial yield stress and r_b were conducted in order to derive anisotropic coefficients *F, G, H, N,* α_{1-8} of Hill-48 and Yld2000-2d model respectively in sheet plane at five ε^p levels. The uniaxial true stress σ_0 and the plastic work per unit volume w^p, associated with a particular value of a true plastic strain ε_0, were determined in reference RD test $\sigma_{ref}(\varepsilon_{ref}{}^p) = \sigma_0(\varepsilon_0{}^p)$. The directional yield stresses are compared at equal plastic stress-work density according to

$$w^p = \int \sigma_0(\varepsilon_0{}^p) d\varepsilon_0{}^p = \int \sigma_{45}(\varepsilon_{45}{}^p) d\varepsilon_{45}{}^p = \int \sigma_{90}(\varepsilon_{90}{}^p) d\varepsilon_{90} \tag{20}$$

The anisotropic coefficients *F, G, H, and N* of Hill-48 model were obtained from equation 4 and using equation 21 to computed r-values.

$$r_0 = \frac{H}{G}, \qquad r_{45} = \frac{2N - (F+G)}{2(F+G)}, \qquad r_{90} = \frac{H}{F} \tag{21}$$

The w^p-levels were graphically transformed to plastic strain levels by simply seeking the plastic strain values and w^p-values that correspond to the same yield stresses in figures 5 and 6. Uniaxial stresses were normalized by the uniaxial stresses in the RD for different amounts of plastic work per unit volume w^p, are listed in table 6 and the values of anisotropic parameters of Hill-48 and corresponding *r-values* are tabulated in table7. The values of anisotropic parameters of Yld2000-2d model are given in table8. At each plastic strain-level the parameters α_{1-8} were calculated using the Newton-Raphson iteration method.

Table 6. The normalized uniaxial stresses in terms of the plastic work per unit volume w^p

w^p [MPa]	$\bar{\varepsilon}(-)$	σ_0 [MPa]	σ_{45} [MPa]	σ_{90} [MPa]	σ_0/σ_0	σ_{45}/σ_0	σ_{90}/σ_0	σ_b/σ_0
0	0	259	263	251	1	1.015	0.969	0.984
115	0.28	506	534	527	1	1.055	1.041	1.023
252	0.52	631	659	668	1	1.044	1.058	1.030
460	0.82	758	786	815	1	1.040	1.075	1.038
587	0.98	819	846	887	1	1.032	1.083	1.041

Note that the equibiaxial yield stress σ_b was assumed in this work. Thus, $\sigma_b = (\sigma_0 + \sigma_{90})/2$

Table 7. The values of anisotropic parameters of Hill-48 and corresponding *r-values*

$\bar{\varepsilon}(-)$	F	G	H	N	r_0	r_{45}	r_{90}	r_b
0	0.48	0.54	0.51	1.41	0.94	0.87	1.06	1.00
0.28	0.51	0.44	0.48	1.31	1.09	0.87	0.93	1.00
0.52	0.52	0.41	0.47	1.36	1.13	0.94	0.90	1.00
0.82	0.53	0.40	0.47	1.40	1.18	1.00	0.88	1.00
0.98	0.53	0.39	0.46	1.41	1.20	1.03	0.87	1.00

Note that the equibiaxial r_b-value was assumed $r_b = 1$.

Table 8. The values of anisotropic parameters of Yld2000-2d function

w^p [MPa]	$\bar{\varepsilon}(-)$	α_1	α_2	α_3	α_4	α_5	α_6	α_7	α_8	k
0	0	0.9222	1.1107	1.0173	1.0154	1.0152	1.0190	0.9777	0.9678	6
115	0.28	1.0995	0.8632	0.9770	0.9775	0.9773	0.9786	0.9405	0.9309	6
252	0.52	1.1409	0.8089	0.9723	0.9689	0.9680	0.9790	0.9542	0.9489	6
460	0.82	1.1817	0.7573	0.9658	0.9593	0.9574	0.9811	0.9614	0.9547	6
587	0.98	1.1997	0.7343	0.9643	0.9551	0.9528	0.9836	0.9696	0.9698	6

The according parameters are given in table 7 and 8, the values of anisotropic parameters of Hill-48 and Yld2000-2d of DIN 1623 St14 steel were calculated using stress ratio and *r-values* in each equivalent plastic strain in figure 7. The values the constants are monotonically with increase of the equivalent plastic strain, except that α_1 and α_2 for Yld2000-2d.

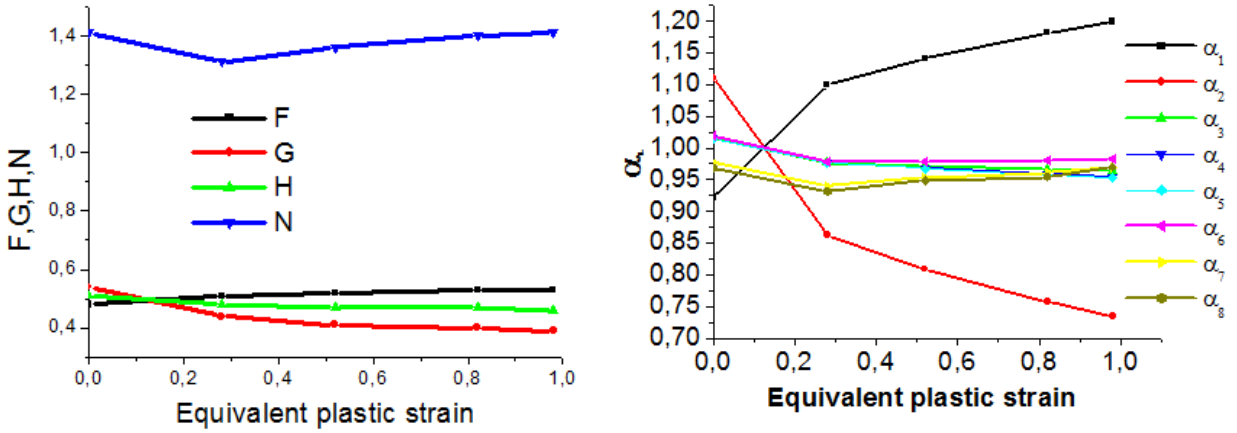

Fig. 7. Anisotropic coefficients were calculated using values of tables 6 and 7

The anisotropy coefficients listed in tables 7 and 8 were used to plot the diagrams in figures 8. Subsequently, the evolution of normalized mechanical parameters of flow stresses $\sigma\ (\theta)$ and Lankford coefficient r (θ) for seven orientations is plotted at five levels of effective plastic strain ε_0^p (which is proportional of specific plastic work w^p per unit volume). Thus, it is graphically demonstrated that the evolution of these parameters based on both yield functions (Hill48 and Yld2000-2d) change with level of ε_0^p at different orientations and the mechanical response is appreciably significant.

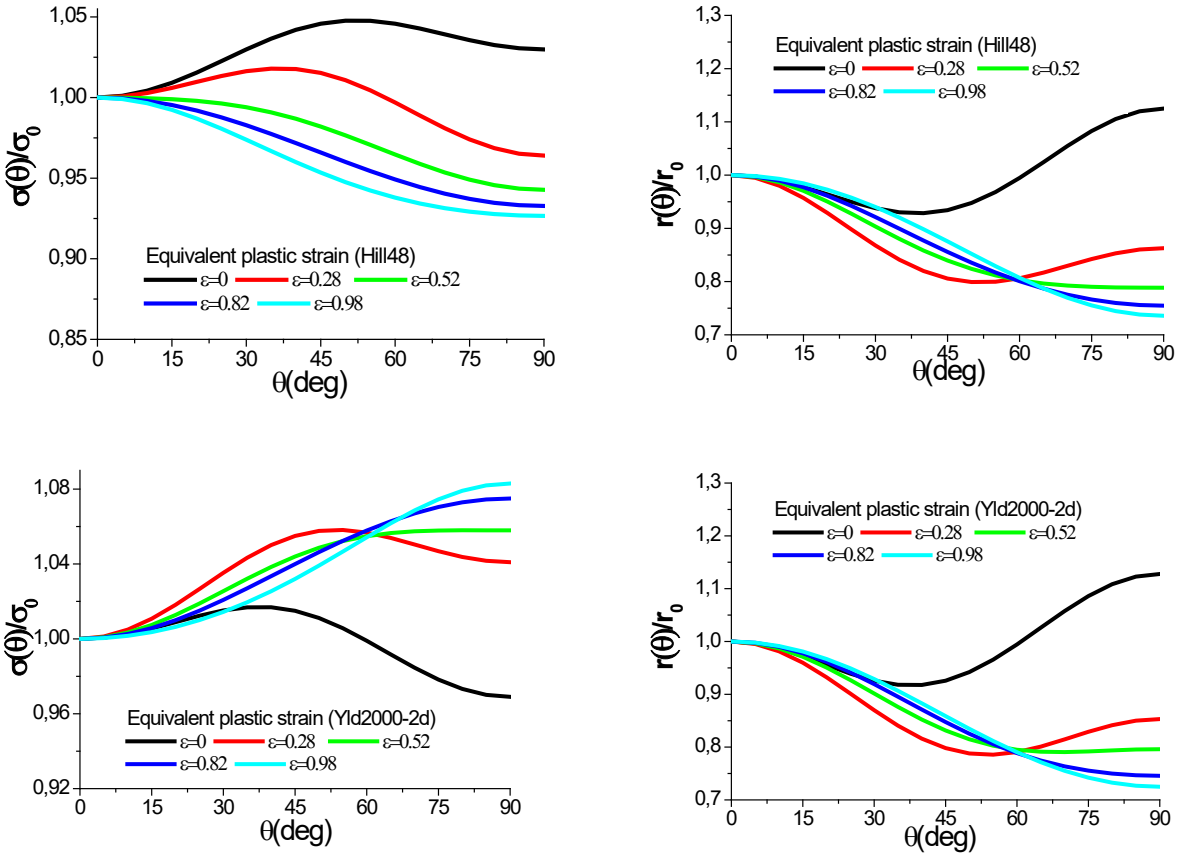

Fig.8. Normalized flow stresses $\sigma\ (\theta)$ and Lankford r (θ) for seven orientations at five levels of effective plastic strain based on both yield functions (Hill48 and Yld2000-2d)

Using Hill-48 and Yld2000-2d criterion, the normalized yield surfaces at different amounts of specific plastic work are shown in figure 9. Yield stress ($\sigma_{11} = \sigma_{RD}, \sigma_{22} = \sigma_{TD}$) presenting a contour of plastic work for a specific value of equivalent longitudinal strain ε_{11} which is converted to $\bar{\varepsilon}^p(0°)$

at $\sigma_{12}=0$, are normalized by the unidirectional tensile flow stress σ_0 corresponding to the $\bar{\varepsilon}^p(0°)$. The figures indicate that the evolutionary of anisotropy as the plastic work changes with the equivalent plastic strain for both functions in the yield surface shape. This suggests that DIN 1623 St14 steel has a tendency to lose its anisotropy at a higher plastic work. Although the shape of the two dimensional sections of the yield surfaces appears influenced, an effect of mechanical behavior can be still visible in other characteristics of sheet plane plastic anisotropy.

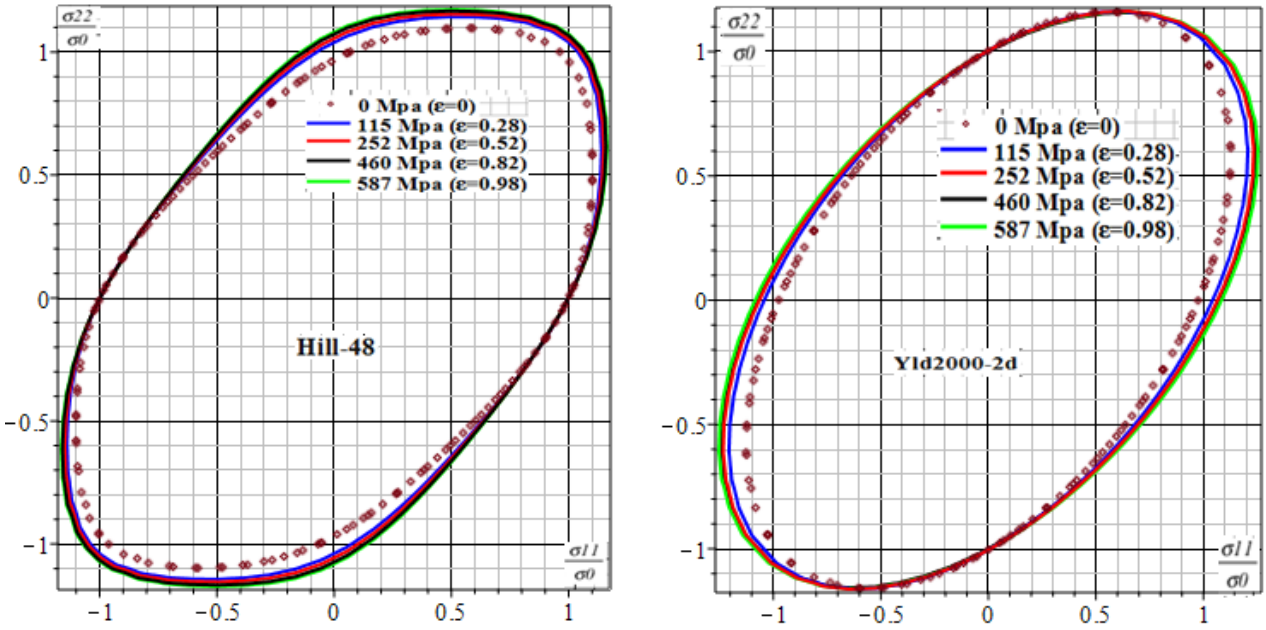

Fig. 9. Normalized yield surfaces predicted with Hill-48 and Yld2000-2d at different amounts of plastic work at $\sigma_{12}=0$

In order to compare this yield surface to an anisotropic yield surface, the normalized shear yield stress is represented by its isoshear contours. The figure 10 shows the yield surface of Hill-48 and Yld2000-2d criterion represented as contours of the normalized shear stress $\sigma_{12}/\sigma_0 = 0, 0.1, 0.2, 0.3, 0.4$ projected onto the normal stress plane (σ_{11}/σ_0, σ_{22}/σ_0). It can be seen from Fig. 10(a)–(c), that the normalized shear stress (σ_{22}/σ_0) applied less influence on the yield surfaces predicted by the Yld2000-2d yield model, but had a greater effect on the Hill-48 yield criterion. To the highest value of normalized shear stress (0.4), both results of Hill-48 yield function and the isotropic behavior described by Von Mises function are almost superimposed. The maximum theoretical value computed of normalized shear stress is (0.5953 where $\sigma_{12}=153.58\ Mpa$) for Hill-48 function but is set at (0.4 where $\sigma_{12}=103.2 Mpa$) for the Yld2000-2d yield model. Generally the shear stress value is often equal to 60% of the yield flow stress σ_0 in uniaxial tensile test, what is closest to Hill-48 criterion, so, it is much recommended to characterize experimentally the sheet by a shear test to determine the real value of σ_{12}. The coefficients of this particular yield function are listed in table 7 and 8 witch according to $\varepsilon_0^p=0$ and $w=0$. Von Mises criterion, Hill-48 and Yld2000-2d criteria led to the similar deviation.

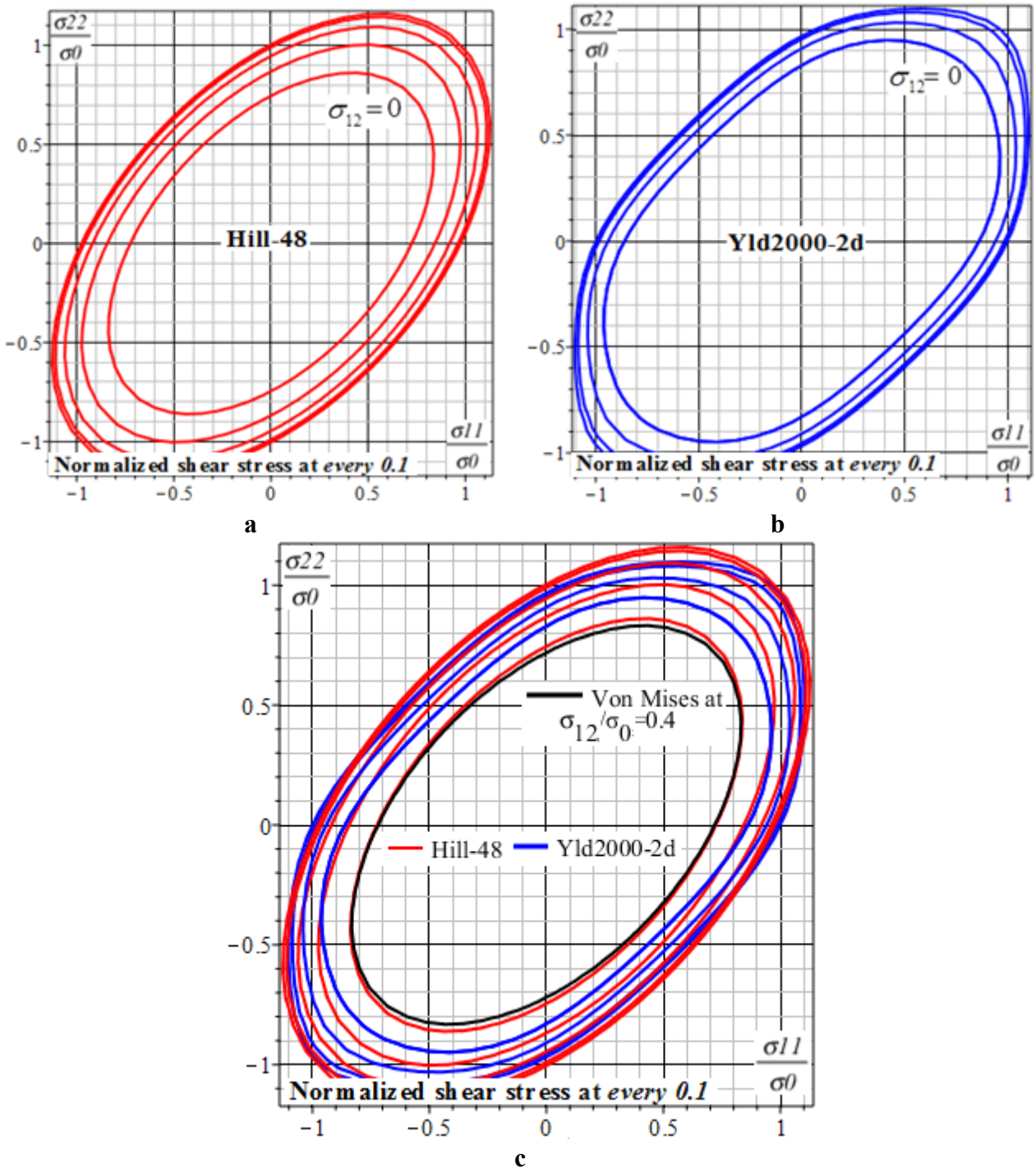

Fig. 10. The calculated yield surface represented by contours of the normalized shear stress at *every 0.1.* (a) Hill-48 yield function, (b) Yld2000-2d yield function and (c) comparison of the predicted yield surface loci

4. Conclusion

In this paper, uniaxial tension in different directions were performed on DIN 1623 St14 steel. Two yield criteria, Hill1948 (quadratic) and Yld2000-2d (non-quadratic) were used to predict flow stresses, *r- values* and to determine the yield surface shapes at different amounts of plastic work. Since the calculated anisotropy coefficients of Hill'48 function only obtained from the input data of the uniaxial yield stress $\sigma_0, \sigma_{45}, \sigma_{90}$ at 0°, 45°, 90° to the RD and equibiaxial tensile stress σ_b. In several points of experience, Yld2000 criterion give better agreement of flow stresses predictions and *r-value* anisotropies with experimental data than the from Hill'48 function. Moreover, the anisotropy

parameters for Hill's 1948 and Barlat's Yld2000-2d yield function were computed as a function of the equivalent plastic strain. The isotropic hardening function is also using to descript the following various empirical standard models and it is shown that a good fit is achieved by Ludwick's model. In addition, the effect of the normalized shear stress projected onto the normal stress plane was discussed in this paper.

Appendix 1

Uniaxial tension test

The rotation of matrix $\boldsymbol{P}$ from the specimen ($\boldsymbol{S}$) to the sheet axes ($\boldsymbol{R}$) and the transposed matrix $\boldsymbol{P^T}$.

$$\boldsymbol{P} = \begin{bmatrix} \cos\theta & -\sin\theta & 0 \\ \sin\theta & \cos\theta & 0 \\ 0 & 0 & 1 \end{bmatrix}, \quad \boldsymbol{P}^T = \begin{bmatrix} \cos\theta & \sin\theta & 0 \\ -\sin\theta & \cos\theta & 0 \\ 0 & 0 & 1 \end{bmatrix} \tag{I.1}$$

Gives the stress tensor in the new reference axes ($\boldsymbol{R}$)

$$\sigma_R = P\sigma_S P^T = \begin{bmatrix} \cos\theta & \sin\theta & 0 \\ -\sin\theta & \cos\theta & 0 \\ 0 & 0 & 1 \end{bmatrix} \begin{bmatrix} \sigma & 0 & 0 \\ 0 & 0 & 0 \\ 0 & 0 & 0 \end{bmatrix} \begin{bmatrix} \cos\theta & -\sin\theta & 0 \\ \sin\theta & \cos\theta & 0 \\ 0 & 0 & 1 \end{bmatrix}$$

$$\sigma_R = \begin{bmatrix} \sigma\cos^2\theta & -\sigma\cos\theta\sin\theta & 0 \\ -\sigma\cos\theta\sin\theta & \sigma\sin^2\theta & 0 \\ 0 & 0 & 0 \end{bmatrix} \tag{I.2}$$

From Hill criterion, it can be written

$$\sigma_0^2 = F\sigma^2\sin^4\theta + G\sigma^2\cos^4\theta + H\sigma^2\cos^2 2\theta + 2N\sigma^2\sin^2\theta\cos^2\theta \tag{I.3}$$

A directional yield stress of specimen under uniaxial tensile test $\sigma(\theta)$ is

$$\sigma(\theta) = \frac{\sigma_0}{\left(F\sin^4\theta + G\cos^4\theta + H\cos^2 2\theta + 2N\sin^2\theta\cos^2\theta\right)^{1/2}} \tag{I.4}$$

Application of the normality rule to the yield equation

$$\dot{\varepsilon}_{ij} = \dot{\lambda}\frac{\partial f(\sigma_{ij})}{\partial\sigma_{ij}} \quad \dot{\lambda} \geq 0 \tag{I.5}$$

Plastic strain increments can be written as a function of the gradient of the yield function:

$$\varepsilon_{ij} = \dot{\lambda}\begin{bmatrix} \dfrac{\partial f(\sigma_{ij})}{\partial\sigma_{xx}} & \dfrac{\partial f(\sigma_{ij})}{\partial\sigma_{xy}} & 0 \\ \dfrac{\partial f(\sigma_{ij})}{\partial\sigma_{yx}} & \dfrac{\partial f(\sigma_{ij})}{\partial\sigma_{yy}} & 0 \\ 0 & 0 & -\left(\dfrac{\partial f(\sigma_{ij})}{\partial\sigma_{xx}} + \dfrac{\partial f(\sigma_{ij})}{\partial\sigma_{yy}}\right) \end{bmatrix} \tag{I.6}$$

Wherefrom:

$$\dot{\varepsilon} = 2\dot{\lambda}\sigma\left[F\sin^4\theta + G\cos^4\theta + H\cos^2 2\theta + (N/2)\sin^2 2\theta\right]$$
$$\dot{\varepsilon}_{yy} = 2\dot{\lambda}\sigma\left[(F+G)\sin^2\theta\cos^2\theta - H\cos^2 2\theta - (N/2)\sin^2 2\theta\right]$$
$$\dot{\varepsilon}_{zz} = -2\dot{\lambda}\sigma\left[F\sin^2\theta + G\cos^2\theta\right]$$
$$\dot{\varepsilon}_{xy} = 2\dot{\lambda}\sigma\left[F\sin^2\theta\sin 2\theta - G\cos^2\theta\sin 2\theta - 2H\cos 2\theta\sin 2\theta + N\sin 2\theta\cos 2\theta\right]$$

Then, the related set of strain rate ratios can be written as follows:

$$\frac{\dot{\varepsilon}_{yy}}{\dot{\varepsilon}} = \frac{2(F+G)\sin^2\theta\cos^2\theta - 2H\cos^2 2\theta - N\sin^2 2\theta}{2F\sin^4\theta + 2G\cos^4\theta + 2H\cos^2 2\theta + N\sin^2 2\theta}$$

$$\frac{\dot{\varepsilon}_{zz}}{\dot{\varepsilon}} = -\frac{2F\sin^2\theta + 2G\cos^2\theta}{2F\sin^4\theta + 2G\cos^4\theta + 2H\cos^2 2\theta + N\sin^2 2\theta}$$

$$\frac{\dot{\varepsilon}_{xy}}{\dot{\varepsilon}} = \frac{(F\sin^2\theta - G\cos^2\theta)\sin 2\theta - (2H-N)\sin 2\theta\cos 2\theta}{F\sin^4\theta + G\cos^4\theta + H\cos^2 2\theta + 2N\sin^2\theta\cos^2\theta}$$

Hence, strain rate ratio $r(\theta)$ in the plane sheet is:

$$r(\theta) = \frac{\dot{\varepsilon}_{yy}}{\dot{\varepsilon}_{zz}} = \frac{\left[H\cos^2 2\theta - (F+G-2N)\cos^2\theta\sin^2\theta\right]}{F\sin^2\theta + G\cos^2\theta} \tag{I.7}$$

Appendix 2

The eight input data are the yield stresses and r- values measured in three different directions of the sheet from uniaxial tension tests, $\sigma_0, \sigma_{45}, \sigma_{90}, r_0$ and r_{90}. The other two data are the balanced biaxial flow stress σ_b and biaxial Lankford value r_b. This system consists of four yield equations for the flow stresses and their corresponding derivatives for the r-values in both uniaxial and biaxial.

$$f_i = \phi - 2\left(\frac{\sigma_0}{\sigma_i}\right)^K = 0$$

$$f_i = \left|\alpha_1\gamma_i - \alpha_2\delta_i\right|^K + \left|\alpha_3\gamma_i + 2\alpha_4\delta_i\right|^K + \left|2\alpha_5\gamma_i + \alpha_6\delta_i\right|^K - 2\left(\frac{\sigma_0}{\sigma_i}\right)^K = 0 \tag{II.1}$$

$$f_4 = \left|\frac{\sqrt{M_2'^2 + 4\alpha_7^2}}{2}\right|^K + \left|\frac{3M_1'' - \sqrt{M_2''^2 + 4\alpha_8^2}}{4}\right|^K + \left|\frac{3M_1'' + \sqrt{M_2''^2 + 4\alpha_8^2}}{4}\right|^K - 2\left(\frac{\sigma_0}{\sigma_{45}}\right)^K = 0 \tag{II.2}$$

$$\begin{aligned} g_i &= (\alpha_1 q_{xi} + \alpha_2 q_{yi})(\alpha_1\gamma_i - \alpha_2\delta_i)\left|\alpha_1\gamma_i - \alpha_2\delta_i\right|^{K-2} + \\ &+ (\alpha_3 q_{xi} - 2\alpha_4 q_{yi})(\alpha_3\gamma_i + 2\alpha_4\delta_i)\left|\alpha_3\gamma_i + 2\alpha_4\delta_i\right|^{K-2} + \\ &+ (2\alpha_5 q_{xi} - \alpha_6 q_{yi})(2\alpha_5\gamma_i + \alpha_6\delta_i)\left|2\alpha_5\gamma_i + \alpha_6\delta_i\right|^{K-2} = 0 \end{aligned} \tag{II.3}$$

$$g_4 = H_1 \frac{M_2'^2}{\sqrt{M_2'^2 + 4\alpha_7^2}} + \frac{3}{2} M_1''(H_2 + L) + \frac{1}{2} \frac{M_2''^2}{\sqrt{M_2''^2 + 4\alpha_8^2}} (L - H_2) - \frac{2K}{(1+r45)} \left(\frac{\sigma_0}{\sigma_{45}} \right)^K = 0 \quad \text{(II.4)}$$

There are three equations for each f_i and g_i corresponding to $i = 1, 2, 3$. In each equation, the values of $\gamma_i, \delta_i, q_{xi}, q_{yi}, \sigma_i, q_{xi}$ and q_{yi} are given in table 9 for the corresponding i. The other expressions needed in f_4 and g_4 are

$$\begin{cases} M_2' = \dfrac{\alpha_1 - \alpha_2}{3} \\ M_1'' = \dfrac{\alpha_3 + 2\alpha_4 + 2\alpha_5 + \alpha_6}{9} \\ M_2'' = \dfrac{2\alpha_5 + \alpha_6 - \alpha_3 - 2\alpha_4}{3} \end{cases}$$

And

$$\begin{cases} H_1 = K \left(\dfrac{\sqrt{M_2'^2 + 4\alpha_7^2}}{2} \right)^{K-1} \\ H_2 = K \left(\dfrac{3M_1'' - \sqrt{M_2''^2 + 4\alpha_8^2}}{4} \right) \left| \dfrac{3M_1'' - \sqrt{M_2''^2 + 4\alpha_8^2}}{4} \right|^{K-2} \\ L = K \left(\dfrac{3M_1'' + \sqrt{M_2''^2 + 4\alpha_8^2}}{4} \right) \left| \dfrac{3M_1'' + \sqrt{M_2''^2 + 4\alpha_8^2}}{4} \right|^{K-2} \end{cases}$$

Table 9. The definition of $\gamma_i, \delta_i, q_{xi}, q_{yi}, \sigma_i, q_{xi}$ and q_{yi} parameters in uniaxial RD, TD and biaxial conditions

Mode	Index i	γ_i	δ_i	σ_i	q_{xi}	q_{yi}
0° Tension	1	2/3	-1/3	σ_0	$1 - r_0$	$2 + r_0$
90° Tension	2	-1/3	2/3	σ_{90}	$2 + r_{90}$	$1 - r_{90}$
Balanced biaxial tension	3	-1/3	-1/3	σ_b	$2 + r_b$	$2 + r_b$

References

[1] W. Liu, D. Guines, L. Leotoing, E. Ragneau, Identification of sheet metal hardening for large strains with an in-plane biaxial tensile test and a dedicated cross specimen, International Journal of Mechanical Sciences. 101–102 (2015): 387-398.

[2] O. Chahaoui, ML. Fares, D. Piot, F. Montheillet., Mechanical Modeling of Macroscopic Behavior for Anisotropic and Heterogeneous Metal Alloys; Met. Mater. Int., 19 (2013) 1005-1019.

[3] O. Chahaoui, ML. Fares, D. Piot, F. Montheillet., Monoclinic effects and orthotropic estimation for the behaviour of rolled sheet, J Mater Sci, 46: 5(2011)1655-1667

[4] L.A.I Kestens, H. Pirgazi.'' Texture formation in metal alloys with cubic crystal structures''. Materials Science and Technology. Vol 32 No 13 (2016) 1303.

[5] R. Hill, A theory of yielding and plastic flow of anisotropic materials. Proceedings: Mathematical, Physical and Engineering Science, Royal Society London, A193 (1948) 281-297.

[6] W.F. Hosford, A generalized Isotropic Yield Criterion.J. Appl. Mech. 39 (1972) 607–609.

[7] F. Barlat, J. Lian, Plastic behavior and stretchability of sheet metals: Part I. A yield function for orthotropic sheets under plane stress conditions. International Journal of Plasticity, 5(1989) 51-66.

[8] Barlat, F., Lege, D. J., and Brem, J. C.: A six-component yield function for anisotropic materials. International Journal of Plasticity, 7, (1991) 693-712

[9] F. Barlat, R.C. Becker, Y. Hayashida, Y. Maeda, M. Yanagawa, K. Chung, J.C. Brem, D.J. Lege, K. Matsui, S.J. Murtha, S. Hattori, Int. J. Plast. 13 (1997) 385–401.

[10] F. Barlat, Y. Maeda, K. Chung, M. Yanagawa, J.C. Brem, Y. Hayashida, D.J. Leged,

K. Matdui, S.J. Murtha, S. Hattori, R.C. Becker, S. Makosey, J. Mech. Phys. Solids 45 (1997) 1727–1763.

[11] F. Barlat, J.C. Brem, J.W. Yoon, K. Chung, R.E. Dick, D.J. Lege, F. Pourboghrat, S.H. Choi, E. Chu, Int. J. Plast. 19 (2003) 1297–1319.

[12] F. Barlat, H. Aretz, J. W Yoon, M.E. Karabin, J.C. Brem, R.E. Dick, Int. J. Plast. 21 (2005) 1009–1039.

[13] Zhang S, Leotoing L, Guines D, Thuillier S, Zang S.l. Calibration of anisotropic yield criterion with conventional tests or biaxial test', International Journal of Mechanical Sciences, 85: (2014)142-151

[14] Farhad Haji Aboutalebi '' Numerical and Experimental Determination of Forming Limit Diagram for DIN 1623 St14 Steel'' steel research int. 81 (2010) No. 9, p 667-669

[15] R. Hill (1950), the Mathematical Theory of Plasticity, Oxford University Press

[16] H. Aretz,' Numerical analysis of diffuse and localized necking in orthotropic sheet metals' International Journal of Plasticity 23 (2007) 798–840.

[17] O. Cazacu, F. Barlat, Generalization of Drucker's yield criterion to orthotropy. Mathematics and Mechanics of Solids 6 (2001) 613–630.

[18] M. Kawka,, A. Makinouchi, Plastic anisotropy in FEM analysis using degenerated solid element. Journal of Materials Processing Technology 60 (1996) 239–242.

[19] Taejoon Park, Kwansoo Chung, Non-associated flow rule with symmetric stiffness modulus for isotropic-kinematic hardening and its application for earing in circular cup drawing, International Journal of Solids and Structures 49 (2012) 3582–3593.

[20] F. Barlat, W.J. Yoon, O. Cazacu, On linear transformations of stress tensor for the description of plastic anisotropy, Int. J. Plast., 23 (2007) 876-896

[21] O. Dion-Martin, M. Fafard, R. Ahmed, G. D'Amours, Characterization of aa5754 alloy for identification of barlat's yld2000-2d yield criterion, (Characterization of Minerals, Metals, and Materials Society, 2013.

[22] T. Kuwabara, F. Sugawara, Multiaxial tube expansion test method for measurement of sheet metal deformation behavior under biaxial tension for a large strain range, International Journal of Plasticity 45 (2013) 103–118.

[23] R. Hill, R., Hutchinson, J. W. Differential hardening in sheet metal under biaxial loading: a theoretical framework, J. Appl. Mech., 59, 2S, S1 (1992)S9,

[24] R. Hill, S.S. Hecker, M.G. Stout, An investigation of plastic flow and differential work hardening in orthotropic brass tubes under fluid pressure and axial load, Int. J. Solids Struct., 31, 21, (1994) 2999–3021,

[25] T. kuwabara, k. ichikawa 'hole expansion simulation considering the differential hardening of a sheet metal' Ro. J. Techn. Sci. − Appl. Mechanics, Vol. 60, Nos 1−2, (2015)63−81, Bucharest.

[26] H. Aretz 'A simple isotropic-distortional hardening model and its application in elastic–plastic analysis of localized necking in orthotropic sheet metals' International Journal of Plasticity 24 (2008) 1457–1480